High Pressure O-17 Longitudinal Relaxation Time Studies in Supercooled H_2O and D_2O

E. W. Lang and H.-D. Lüdemann

Institut für Biophysik und Physikalische Biochemie, Universität Regensburg, Postfach 397, D-8400 Regensburg

Flüssigkeiten / Hohe Drücke / Magnetische Kernresonanz / Transporterscheinungen / Zwischenmolekulare Wechselwirkungen

The spin-lattice relaxation times T_1 of the oxygen-17 isotope in light and heavy water have been measured at 13.56 MHz in the temperature range 457 K to 238 K and up to pressures of 250 MPa. Below 300 K all isotherms exhibit maxima of T_1 which become most pronounced at the lowest temperatures measured. A marked isotope effect is seen in going from light to heavy water. The ratio $[T_1(H_2{}^{17}O)/T_1(D_2{}^{17}O)]_{T,p}$ is temperature dependent and increases with decreasing temperature. Furthermore the isotherms in $D_2{}^{17}O$ exhibit a stronger pressure dependence than the isotherms in $H_2{}^{17}O$. The correlation times τ_θ derived from ^2H-T_1 and ^{17}O-T_1 in heavy water are identical at all pressures and temperatures and demonstrate the isotropic nature of the orientational fluctuations of the molecules in liquid water. The temperature dependence of τ_θ can at low pressures ($p < 150$ MPa) be described by a fractional power law with a singular temperature T_s, whereas at high pressure ($p > 150$ MPa) the isobars can only be fitted by the VTF-equation with the ideal glass transition temperature T_0. T_s as well as T_0 are found to be higher in heavy water compared to light water.

Introduction

Liquid water at temperatures $T \leq 300$ K has many unusual physical properties, which in their combination are found in this liquid only. Some examples for these anomalies are the temperature of maximum density ($T_{MD} = 277$ K in H_2O resp. 284 K in D_2O) and the compressibility minimum around 320 K. Application of hydrostatic presssure leads at temperatures < 300 K to an initial increase of the mobility of liquid water. A minimum in the viscosity-isotherms and a maximum in the self-diffusion coefficient-isotherms is observed in the pressure range between 0.1 and 200 MPa [1]. Since all these anomalies are most pronounced in the vicinity of the melting pressure curve it appears desirable to extend the study of the properties of liquid water into the metastable supercooled range. In the last years a variety of physical properties of supercooled water has been studied by Angell and collaborators [1]. The experimental difficulties in studying supercooled water are significantly reduced when it is possible to apply the measurements to water emulsions [2].

NMR-measurements can take full advantage of this emulsion technique and thus the spin-lattice relaxation times T_1 of the protons in light water and the deuterons in heavy water are to our knowledge the only properties that could be measured at pressures up to 300 MPa down to the homogeneous nucleation temperature [3, 4]. These studies revealed that the anomalous pressure dependence of the T_1-isotherms becomes much more pronounced in the supercooled region and showed qualitatively that the substitution of the protons by the deuterons in going from light to heavy water must influence the pressure – as well as the temperature dependence of the correlation times. In order to study this isotope effect more quantitatively, oxygen-17 studies in H_2O and D_2O enriched with this isotope were performed.

Experimental

The spin-lattice relaxation times of the oxygen-17 nucleus were obtained at 13.56 MHz on a Varian XL-100-15 FT NMR-spectrometer equipped with a high power pulse amplifier and interfaced to a 16 K Varian 620-l-100 computer by a $\frac{\pi}{2} - T - \pi - \tau - \frac{\pi}{2}$ pulse sequence. The emulsions were contained in a high pressure glass capillary with i.d. 1.2 mm and o.d. 7 mm. Details of the high pressure equipment have been described elsewhere [5, 6]. The pressures extend to 250 MPa. They were measured by a precision Bourdon gauge (Heise, Newton, CT, USA) to ±0.5 MPa and generated with standard $(\frac{1}{8})''$ equipment (HIP, Erie PA, USA). The temperatures were determined to ±0.5 K by a chromel-alumel thermocouple. The temperature has been varied from 457 K to 238 K into the supercooled region. Due to electronic limitations of the spectrometer we have not been able to measure T_1 at lower temperatures. The emulsions were prepared from triply destilled light and heavy water enriched to 25% with ^{17}O (GFK-Isotopenstelle, Karlsruhe, BRD) and emulgated in a mixture of 50% w/w methylcyclohexane and 50% w/w methylcyclopentane (E. Merck, Darmstadt, BRD). In order to stabilize the emulsions 4% w/w of an emulgator (Span 65, Serva, Heidelberg, BRD) were added to the cycloalkanes. The components were degassed carefully in the sample container (Fig. 1A) on a high vacuum line by at least five freeze-pump-thaw cycles to a final pressure of 7 mPa. The emulsions were prepared after flame sealing the neck of the sample container by rigorously slashing the mixture through a stainless steel net (635 mesh, Spörl & Co., Sigmaringendorf, BRD). In order to fill the high pressure cell, the sealed container with the emulsion was mounted on the filling

Ber. Bunsenges. Phys. Chem. *85*, 603 – 611 (1981) – © Verlag Chemie GmbH, D-6940 Weinheim, 1981.
0005 – 9021/81/0707 – 0603 $ 02.50/0

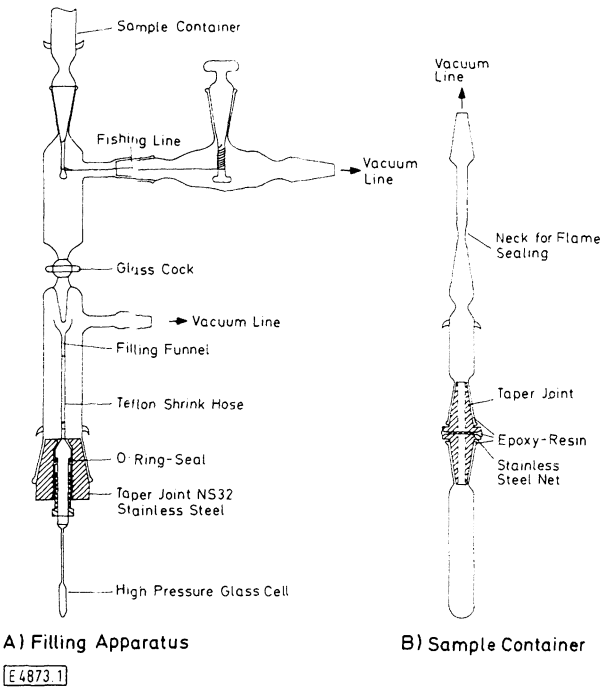

Fig. 1A
Glass apparatus for the filling of the high pressure cells with oxygen free water cycloalkane emulsion

Fig. 1B
Glass ampoule for the preparation oxygen free water cycloalkane emulsions.
During operation the parts given here are connected to a high vacuum line by taper joints. Final pressure: 7 mPa

apparatus (Fig. 1B). After degassing the whole apparatus carefully for at least 24 hours the connections to the vacuum line were closed and the neck of the sample container broken off by winding up of the fishing line. About 1 cm^3 of the emulsion was then allowed to flow into the filling funnel. After the emulsion had filled the pressure cell completely the lower part of the filling apparatus was taken apart and the neck of the filling funnel flame sealed.

Theoretical

The spin-lattice relaxation of the oxygen-17 nucleus is entirely due to its intramolecular quadrupole interaction [7]. The time-dependence of this interaction is caused by the rotational motion of the water molecules. For a nucleus with $I > 1$ (^{17}O: $I = 5/2$) the decay of the resulting spin magnetization does not neccessarily obey the Bloch-equations [8]. However in the fast motional limit the measured spin-lattice relaxation rate T_1^{-1} of the ^{17}O-nucleus is given by

$$T_1^{-1} = \frac{3}{125}\left(\frac{e^2qQ}{h}\right)^2\left(1+\frac{\eta_Q^2}{3}\right)\cdot\tau_\theta \qquad (1)$$

with $\tau_\theta := J(0) = \int_0^\infty G(t)\,dt$ an effective microscopic time constant characterizing the decay of the relevant orientational fluctuations of the molecules. $\frac{e^2qQ}{h}$ and η_Q are the quadrupole coupling constant $C_{17_{O\text{-}QC}}$ of the ^{17}O-nucleus respectively the asymmetry parameter of the electric field gradient q at the nucleus.

Results

Figs. 2 and 3 contain the spin-lattice relaxation times T_1 of the ^{17}O-nucleus between 457 K and 238 K and pressures up to 250 MPa in $H_2{}^{17}O$ and $D_2{}^{17}O$. The data are also compiled in Tables 1 and 2. To the best of our knowledge the pressure dependence of T_1 of the ^{17}O-nucleus

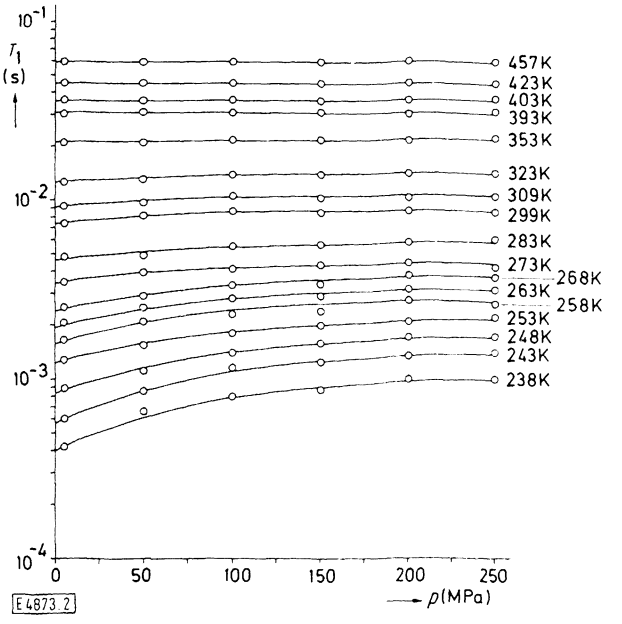

Fig. 2
Pressure and temperature dependence of the longitudinal relaxation times T_1 of the oxygen-17 in H_2O

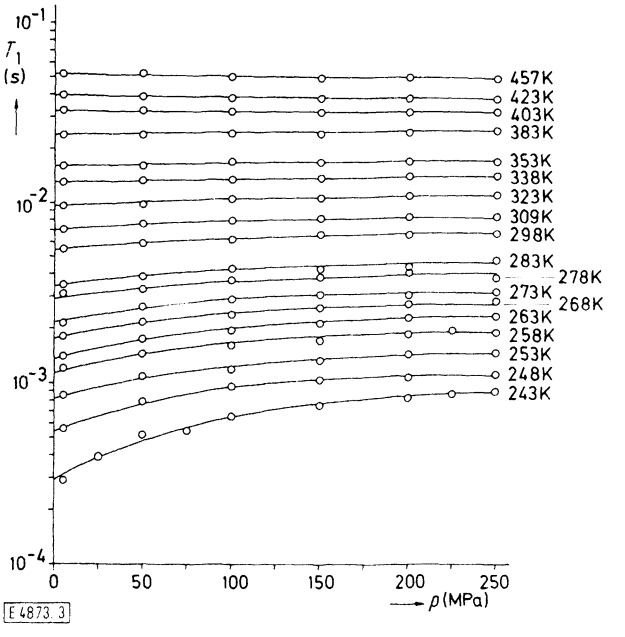

Fig. 3
Pressure and temperature dependence of the longitudinal relaxation times T_1 of the oxygen-17 in D_2O

in water has not been reported in the literature. At normal pressure, however, several authors measured the temperature dependence of the ^{17}O-T_1 in light water [9–13]. Especially Hindman et al. reported T_1 in $H_2{}^{17}O$ to temperatures as low as 242 K [13]. Extrapolation of the data given here at $p = 5$ MPa to $p = 0.1$ MPa and comparison with the older data shows good agreement in the whole temperature range (Table 1). The only older measurement of ^{17}O-T_1 in D_2O [10] found at 302 K identical T_1-values in light and heavy water. This results is in marked disagreement with the results reported in this paper. In the whole pressure- and temperature range studied the ^{17}O-T_1 values are longer in $H_2{}^{17}O$ than in $D_2{}^{17}O$. The ratio $\left(\frac{T_1(H_2{}^{17}O)}{T_1(D_2{}^{17}O)}\right)_{T,p}$ is temperature dependent and increases with decreasing temperatures. Furthermore the pressure dependence of the low temperature T_1-iso-

Table 1
Spin-lattice relaxation times T_1 (ms) of the oxygen-17 nucleus in $H_2{}^{17}O$.

p(MPa) T(K)	5	50	100	150	200	250	0.1 (extrapolated)[a]	0.1 (Ref. [12])[b]	0.1 (Ref. [11])[b]	0.1 (Ref. [13])[b]
457	59	59	59.3	60.7	59.5	59	59	–	60	6[illegible]
423	44.9	44.5	44.1	44.5	44.7	44.7	45	–	45	4[illegible]
403	36	36	35.9	37.4	35.9	37.4	36	–	37	3[illegible]
383	30.3	31.4	30.6	31.2	29.70	31.6	30.5	–	29.2	28.7
353	21.2	21.2	21.6	21.9	21.6	22.5	21	21	20	19.1
323	12.3	13.2	13.7	13.9	13.8	14.2	12.5	12.3	12	1[illegible].6
309	9.29	9.65	10.6	10.2	10.2	10.4	9.2	9.0	9	8.8
299	7.38	8.16	8.59	8.49	8.62	8.49	7.4	7.0	7.1	[illegible].0
283	4.84	4.84	5.46	5.62	5.72	6.08	4.6	4.4	4.5	4.4
273	3.52	3.95	4.09	4.33	4.43	4.22	3.4	3.1	3.2	3.0
268	2.51	2.89	3.33	3.39	3.83	3.74	2.4	2.6	2.6	2.4
263	2.08	2.50	2.83	2.93	3.48	3.16	1.93	2.1	2.1	1.91
258	1.67	2.10	2.29	2.39	2.75	2.62	1.55	1.7	1.6	1.44
253	1.27	1.54	1.82	1.99	2.11	2.18	1.23	–	–	1.05
248	0.88	1.12	1.40	1.59	1.71	1.73	0.83	–	–	0.74
243	0.60	0.86	1.17	1.26	1.35	1.41	0.57	–	–	0.5
238	0.42	0.66	0.80	0.87	1.00	0.99	0.40	–	–	0.32

[a]) Data obtained by extrapolation of the isotherms measured from 5 MPa to 0.1 MPa.
[b]) Data calculated with the resp. fit-equations published by Hindman et al. (Ref. [11 – 13]).

Table 2
Spin-lattice relaxation times T_1 (ms) of the oxygen-17 nucleus in $D_2{}^{17}O$

p(MPa) T(K)	5	50	100	150	200	250	300
457	52	52	50.5	49	49	49	–
423	39.5	38.7	38	38	38	38	–
403	32.5	32.5	32	32	31.2	32.2	–
383	23.7	24.1	25	24.1	24.8	25.6	26.0
353	16.0	16.2	17.0	16.9	16.9	17.3	17.6
338	13.0	13.4	13.4	13.7	14.1	14.1	–
323	9.57	9.88	10.6	10.7	11.1	11.3	11.0
309	7.07	7.59	7.90	8.16	8.32	8.22	8.11
298	5.51	5.93	6.24	6.66	6.55	6.66	7.10
283	3.49	3.90	4.27	4.31	4.40	4.80	4.60
278	3.12	3.28	3.69	3.90	4.11	3.80	4.21
273	2.15	2.65	2.90	2.86	3.06	3.10	–
268	1.82	2.17	2.38	2.61	2.73	2.86	–
263	1.41	1.75	1.96	2.15	2.30	2.35	–
258	1.18	1.46	1.63	1.72	1.87	1.90	–
253	0.86	1.08	1.21	1.34	1.44	1.47	–
248	0.56	0.79	0.95	1.05	1.08	1.12	–
243	0.29	0.52	0.68	0.76	0.83	0.90	–

Table 3
Compilation of determined and estimated quadrupole coupling constants $C_{17O\text{-}QC}$ and C_{DQC} from the literature together with the values used in this paper

Phase	C_{DQC}	η	Ref.	C_{17OQC}	η	Ref.
Gas						
HDO	318.6 ± 2.4	0.06 ± 0.16	[39]	10170 ± 70	0.75 ± 0.01	[40]
liquid						
H_2O				(8200 – 7600) ± 200		[12]
				(9000 – 8000)		[9]
				7700 ± 100		[10]
D_2O				7700 ± 100		[10]
supercooled liquid						
D_2O	214 ± 12	≈0	[4]	6600 ± 100	0.93 ± 0.01	[a]
H_2O				6600 ± 100	0.93 ± 0.01	[a]
ice Ih						
H_2O				6525 ± 15	0.925 ± 0.02	[41]
				11330 ± 50	0.06 ± 0.06	[42]
D_2O	213.4 ± 0.3	0.112 ± 0.005	[43]	6600 ± 100	0.935 ± 0.01	[45]
	213.2 ± 0.8	0.100 ± 0.002	[44]	11330 ± 50	0.06 ± 0.06	[42]

[a]) This value has been chosen as the mean of the experimental results in $D_2{}^{17}O$-ice Ih and $H_2{}^{17}O$-ice Ih in accordance with the result found for C_{DQC} in supercooled water [4].

therms is stronger in heavy water than in light water. In the supercooled region the maxima of the ^{17}O-T_1 isotherms are much more pronounced and closely follow the trends observed for the T_1 of the protons and deuterons in the respective liquids [3, 4]. This drastic increase of the mobility after application of pressure has hitherto only been found in liquid water.

Discussion

The Quadrupole Coupling Constant

In order to calculate from the T_1-values measured the correlation times τ_θ the quadrupole coupling constants of the ^{17}O-nucleus ($C_{17_{O\text{-}QC}}$) of the water molecules in the fluid phase is needed. Table 3 compiles available estimates and determinations of $C_{17_{O\text{-}QC}}$ of the water molecules in its different phases. As can be seen from a comparison with C_{DQC} in different phases [4] the $C_{17_{O\text{-}QC}}$ is subject to the same relative reduction ($\sim$35%) in going from the gase phase to the solid state. It is thus to be expected that the $C_{17_{O\text{-}QC}}$ will change with temperature and pressure. However no independent way of determining such a temperature dependence is yet available. The conclusions drawn in the literature range from almost no temperature dependence [12] to a temperature dependence with a minimum at $\sim$310 K [9]. For the C_{DQC} all available experimental evidence indicate a reduction of about 5% of C_{DQC} with decreasing temperature in the range T = 373 K to 273 K and no pressure dependence [14, 15]. A similar change is to be expected in the case of $C_{17_{O\text{-}QC}}$. To a first approximation it appears thus permissible to neglect any pressure- and temperature dependence of the quadrupole coupling constant.

The C_{DQC} of supercooled liquid heavy water was found to be close to the value determined in the low pressure solid phases of water. The $C_{17_{O\text{-}QC}}$ measured for $H_2{}^{17}O$ and $D_2{}^{17}O$ in different ice phases do show no influence of the hydrogen isotope upon this quantity. We therefore choose $C_{17_{O\text{-}QC}}$ = 6.6 ± 0.1 MHz and η_Q = 0.93 ± 0.01 observed in ice Ih as temperature- and pressure independent parameters for light and heavy water to calculate the orientational correlation times τ_θ via Eq. (1) from the experimental ^{17}O-T_1.

Estimate of the Correlation Times

The absolute values of the correlation times τ_θ in $D_2{}^{17}O$ obtained with Eq. (1) exhibit the same pressure- and temperature dependence as those calculated from the ^2H-T_1 [4, 16] as can be seen in Figs. 4 and 5. Whereas the numerical coincidence of the two sets of correlation times depends on the choice of the respective quadrupole coupling constants, their corresponding pressure- and temperature dependence does not. This clearly shows the isotropic character of the orientational fluctuations of the water molecules. Since the main axes systems of the

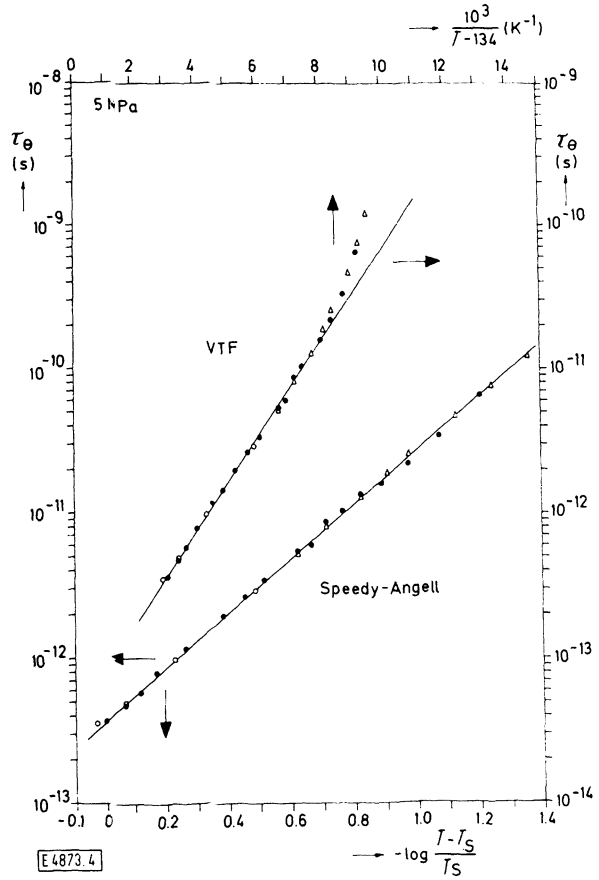

Fig. 4
Representation of the 5 MPa isobar of the orientational correlation times τ_θ for D_2O by the Speedy-Angell and VTF-equation (T_0 = 134 K, T_s = 229 K).
Open circles: τ_θ derived from the ^2_1H-T_1 by Jonas et al. [15, 48].
Open triangles: τ_θ derived from the ^2_1H-T_1 of Ref. [4].
Full circles: τ_θ derived from the $^{17}_8O$-T_1

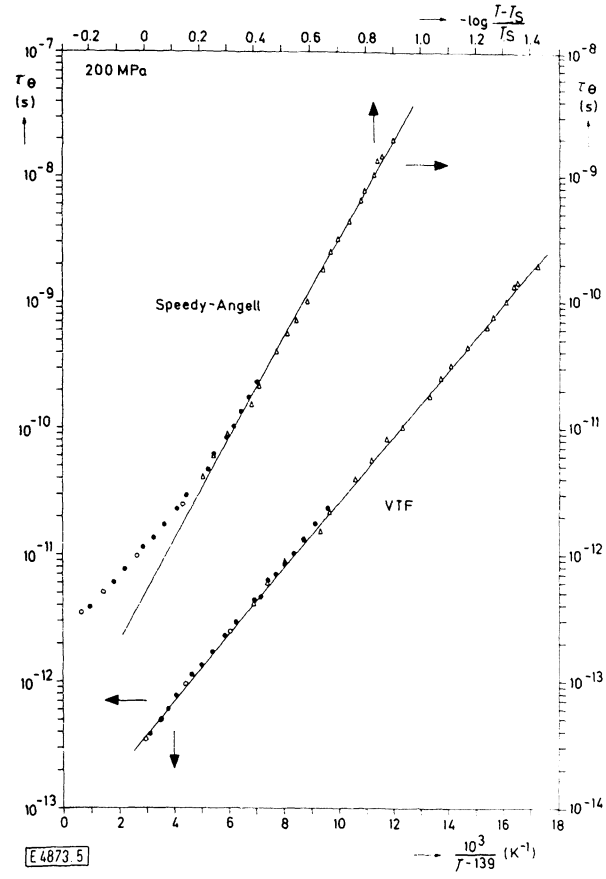

Fig. 5
Representation of the 200 MPa isobar of the orientational correlation times τ_θ for D_2O by the Speedy-Angell and VTF-equation (T_0 = 139 K, T_s = 175 K).
Open circles: τ_θ derived from the ^2_1H-T_1 by Jonas et al. [15, 48].
Open triangles: τ_θ derived from the ^2_1H-T_1 of Ref. [4].
Full circles: τ_θ derived from the $^{17}_8O$-T_1

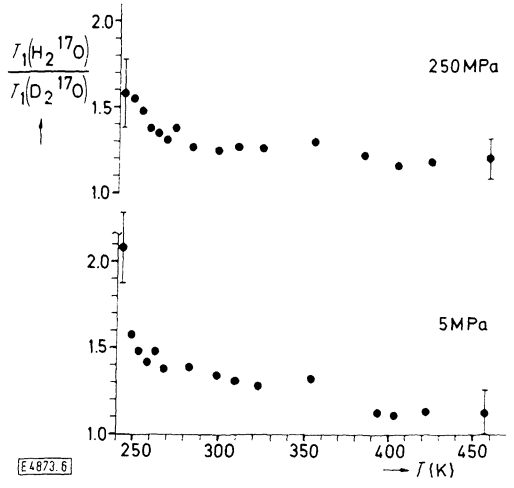

Fig. 6
Ratio of the $^{17}_{8}O$-T_1 obtained in H_2O and D_2O as function of temperature for 5 and 200 MPa

deuterium and oxygen-17 electric field gradient tensors are different in a molecular axis system, anisotropic reorientation of the water molecules should lead to different pressure- and temperature dependences of the relaxation times of ^{17}O and ^{2}H [8, 17]. A comparison of the correlation times τ_θ in $H_2{}^{17}O$ and $D_2{}^{17}O$ shows shorter correlation times in light water than in heavy water. Also the pressure- and temperature dependence of τ_θ is different in $H_2{}^{17}O$ and $D_2{}^{17}O$. The ratio $\left(\frac{T_1(D_2{}^{17}O)}{T_1(H_2{}^{17}O)}\right)_{T,p}$ is thus temperature dependent and is shown in Fig. 6 for 5 MPa and 200 MPa. These results reveal a complicated isotope effect which neither scales with the respective moments of inertia nor with the masses of the two molecules.

Temperature Dependence of the Correlation Times in Light and Heavy Water at Constant Pressure

The correlation times τ_θ derived from ^{17}O-T_1 of heavy water are identical to the results found for the ^{2}H-T_1 (see Figs. 4 and 5). Their temperature dependence can be described by the same equations as the latter [4], i.e. in the low pressure region ($p \leq 150$ MPa) by the singular equation proposed by Speedy and Angell [18] and Anasimov et al. [35]

$$\tau_\theta = \tau_s \cdot \varepsilon^{-\gamma}, \quad \varepsilon = \frac{T - T_s}{T_s} \tag{2}$$

and in the high pressure region ($p \geq 200$ MPa) by the VTF-equation [19–21]

$$\tau_\theta = \tau_0 \exp\left(\frac{B}{T - T_0}\right). \tag{3}$$

The data have been analysed with a least squares fit program. The relevant parameters obtained from this fit are compiled in the Tables 4 and 5. The same analysis has been applied to the correlation times τ_θ derived from the ^{17}O-T_1 in light water. The corresponding parameters are included in Tables 4 and 5 also. The VTF-equation, which applies to water under high hydrostatic pressure, is known to describe successfully the temperature dependence of transport coefficients in many viscous liquids [22, 23]. At the glass transition, characterized through the ideal glass transition temperature T_0 the system reaches a state of lowest potential energy compatible with a fully amorphous arrangement of the molecules [24]. According to the free volume theories of the glass transition [25, 26] the liquid has lost at T_0 all its free volume so that diffusional processes become impossible. The entropy theory of the glass transition [27] identifies T_0 with a state of vanishing configurational entropy of the liquid. The experimentally determined glass transition temperature T_g is for kinetic reasons found always $\sim 10-20$ K above T_0 [1, 23]. The fast crystallization of liquid water prohibited the direct determination of T_g for this substance until now. Measurements of T_g in aqueous binary systems led to an extrapolated glass transition temperature for pure water of T_g (0.1 MPa) = 140 K and T_g (200 MPa) = 146 K in light water [28, 29] and T_g (0.1 MPa) = 144 K in heavy water [29]. In amorphous vapour deposited water a glass transition temperature $T_g \approx 140$ K has been found [30]. From the temperature dependence of the specific heat C_p at constant pressure Kanno and Angell [31] evaluated an ideal glass transition tem-

Table 4
Parameters obtained by least-squares fitting the correlation times τ_θ to Eq. (2)

P (MPa)	$T_s \pm 2$ (K)		$\gamma \pm \sigma_\gamma$		$(\tau_s \pm \sigma_{\tau_s}) \cdot 10^{-13}$ (s)		corr. coef.	
	D_2O	H_2O	D_2O	H_2O	D_2O	H_2O	D_2O	H_2O
0.1	230	223	1.85 ± 0.01	1.89 ± 0.05	3.74 ± 0.1	3.42 ± 0.1	0.9998	0.9991
5	229	221	1.87 ± 0.02	1.87 ± 0.02	3.67 ± 0.2	3.67 ± 0.2	0.9993	0.9993
50	221	215	1.93 ± 0.02	1.96 ± 0.02	4.23 ± 0.1	3.78 ± 0.1	0.9996	0.9997
100	210	204	2.11 ± 0.02	2.11 ± 0.02	4.95 ± 0.1	4.95 ± 0.1	0.9994	0.9992
150	196	189	2.37 ± 0.1	2.56 ± 0.1	6.73 ± 0.2	6.00 ± 0.2	0.9991	0.9978

Table 5
Parameters obtained by a least-squares fit of the correlation times τ_θ to Eq. (3)

P (MPa)	$T_0 \pm 2$ (K)		$B \pm \sigma_B$ (K)		$(\tau_0 \pm \sigma_{\tau_0}) \cdot 10^{-14}$ (s)		corr. coef.	
	D_2O	H_2O	D_2O	H_2O	D_2O	H_2O	D_2O	H_2O
150	137	131	633 ± 3	652 ± 5	6.6 ± 0.3	4.6 ± 0.3	0.9998	0.9996
200	139	134	604 ± 3	623 ± 7	6.1 ± 0.5	4.6 ± 0.5	0.9997	0.9992
250	143	135	563 ± 3	581 ± 5	7.0 ± 0.6	5.9 ± 0.3	0.9997	0.9986

perature T_0 (0.1 MPa) = 130 K in light water, at which the total configurational entropy ($S_{liquid} - S_{ice}$) should be exhausted. The ideal glass transition temperatures T_0 obtained for supercooled light water under high hydrostatic pressure, i.e. T_0 (200 MPa) = 134 K, is ~12 K lower than the experimental T_g [29]. T_0 shows a slight increase with pressure with a pressure coefficient of $\frac{\Delta T_0}{\Delta p} \simeq 0.03 \left(\frac{K}{MPa}\right)$. Extrapolation to atmospheric pressure leads to T_0 (0.1 MPa) = 128 K in H_2O and is in good agreement with the above mentioned value T_0 (0.1 MPa) = 130 K [31]. As can be seen from Table 5, T_0 in D_2O is, compared to H_2O, higher by ~5 K. This isotope effect is in very good agreement with $T_g(D_2O) - T_g(H_2O) = 5$ K found by Kanno et al. [32] for aqueous electrolyte solutions. In D_2O the same pressure coefficient for $T_0(P)$ is found as in H_2O. Extrapolation of $T_0(P)$ to p = 0.1 MPa leads to T_0 (0.1 MPa) = 134 K for D_2O which again is about 10 K below the extrapolated experimental glass transition temperature T_g (0.1 MPa) = 144 K. These results are included in a supplemented phase diagram of light and heavy water in Fig. 7.

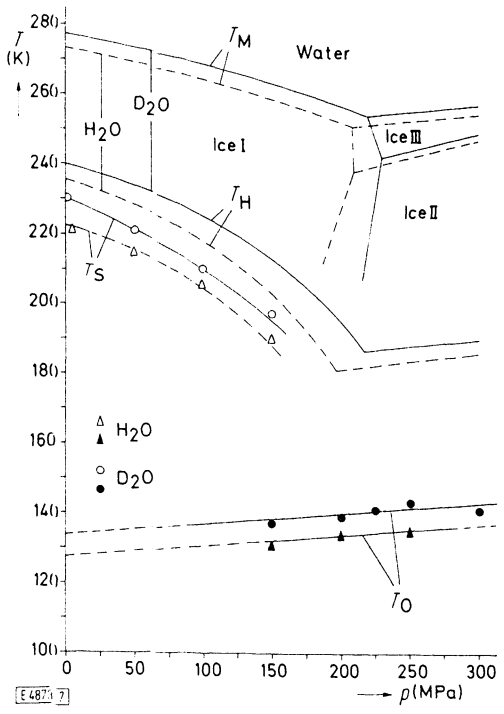

Fig. 7
Part of the phase diagram of H_2O and D_2O showing the pressure and isotope dependence of the homogeneous nucleation temperature T_H, the singular temperature T_s of Eq. (2) and the glass temperature T_0

A marked isotope effect is also seen in the preexponential factor τ_0 of the VTF-equation which upon isotopic substitution scales with the square root of the respective moments of inertia. τ_0 can obviously be converted into a frequency which should yield information about those intra- or intermolecular vibrations whose stochastic excitation and damping influence the orientational correlation times. These frequencies fall into the spectral region of the librational motions of the water molecule in the liquid which also transform with the square root of the moments of inertia upon isotopic substitution [23]. At p = 200 MPa one obtains:

$$\tau_0^{-1}(H_2O) \simeq 725 \text{ cm}^{-1}, \quad \tau_0^{-1}(D_2O) \simeq 547 \text{ cm}^{-1}$$

which leads to

$$\frac{\tau_0^{-1}(H_2O)}{\tau_0^{-1}(D_2O)} \simeq 1.34$$

compared to

$$\left(\frac{I(D_2O)}{I(H_2O)}\right)^{1/2} = 1.38, \quad I\text{-moment of inertia.}$$

It thus seems reasonable to assume that the librational motions control the orientational fluctuations of the water molecules under high hydrostatic pressure ($p \geq 150$ MPa). The collective configurational fluctuations connected with the glass transition appear to dominate the orientational fluctuations which characterize the rotational motions of the molecules in supercooled liquid water in this pressure range.

In the low pressure region ($p \leq 150$ MPa) liquid water shows an anomalous decrease of τ_θ with increasing pressure which becomes much more pronounced in the supercooled region. At low pressures the VTF-equation containing the extrapolated T_0-temperatures discussed above or a T_0 corroborated by any other experimental results [31, 34] fails to describe the temperature dependence of τ_θ. Especially at low temperatures τ_θ increases much faster with decreasing temperature than the VTF-equation would predict (see Fig. 4). As in the case of the deuterium-T_1 [4] the temperature dependence of τ_θ can thus best be accounted for with a fractional power law first proposed by Speedy and Angell [18] and Anasimov et al. [35].

The singular temperature T_s has been interpreted as the boundary of the free energy surface for liquid water or as a line of metastable higher order transitions running across the free energy surface [1]. Table 4 compiles the parameters found for light and heavy water. Table 6 compares the singular temperatures T_s obtained in H_2O and D_2O with estimates taken from the

Table 6
Comparison of the temperatures T_s obtained with data from the literature

p (MPa)	T_s (K) This paper	Ref. [46]	Ref. [47]	Ref. [18]
		H_2O		
0.1	223		225	228
5	221			
10		228		
50	215	224		
100	204	212		
150	189	192		
190		175		

p (MPa)	T_s (K) This paper	Ref. [46]	Ref. [31]
		D_2O	
0.1	230		236
5	229		
10		233	
20			233
50	221	230	226
70			221
100	210	217	211
120			206
150	196	195	200
190		155	

literature. Considering the difficulty of a precise determination of this temperature, the agreement is reasonably good. It should be mentioned that the homogeneous nucleation which occurs ~10 K above T_s limits the experimental data to $\varepsilon \geq 0.05$ and thus excludes the region of ε which in other critical phenomena is most sensitive to the proper choice of the exponent $\gamma(\varepsilon \approx 10^{-4}-10^{-6})$. As can be seen from Table 4 the isotope effect measured in the correlation times τ_θ is at $p \leq 150$ MPa only reflected in the parameter T_s. At equal values of $(T - T_s)$ light and heavy water must therefore have identical correlation times τ_θ. Fig. 8 shows this data reduction for $p = 5$ MPa – $p = 150$ MPa. The pressure dependence of T_s parallels that of the homogeneous nucleation temperature T_H up to $p = 150$ MPa as can be seen from the supplemented phase diagram in Fig. 7.

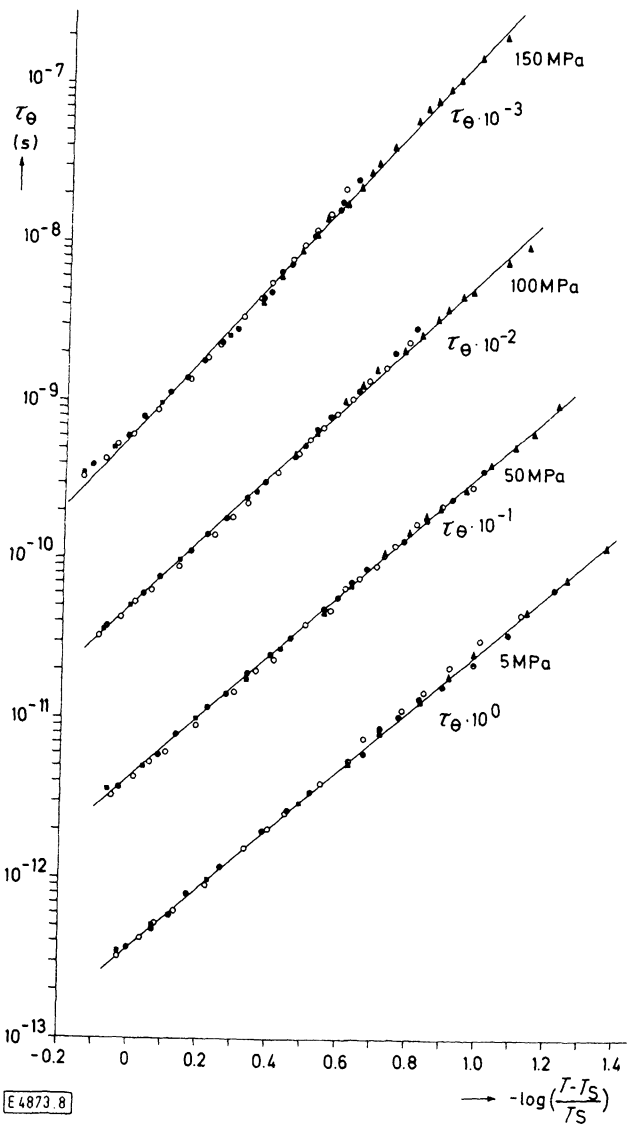

Fig. 8
Representation of the isobars of the correlation times τ_θ in H_2O and D_2O by the reduced temperatures of Table 4. The different isobars have for the sake of clarity been displaced by one order of magnitude.
open circles: τ_θ derived from ^{17}O-T_1 in $H_2{}^{17}O$
full circles: τ_θ derived from ^{17}O-T_1 in $D_2{}^{17}O$
full triangles: τ_θ derived from ^{2}H-T_1 in D_2O of Ref. [4]
full squares: τ_θ derived from ^{2}H-T_1 in D_2O of Jonas et al. [15, 48]

The data indicate that T_s will fall below T_0 in the pressure range $p = 200-250$ MPa. The characteristic frequency τ_s^{-1} corresponding to the preexponential factor τ_s in Eq. (2) falls in the energy spectrum of liquid water into the frequency region of the hydrogen-bond bending motions [33] which transform under isotopic substitution with the square root of the respective molecular masses. The absence of an isotope effect in τ_s larger than the limits of experimental error ($\leq 20\%$) is then readily explained. The identification of the characteristic frequencies τ_s^{-1} with the hydrogen-bond bending motions indicates the nature of the fluctuations connected with the proposed thermodynamic singularity at T_s. These fluctuations produce in the random hydrogen-bonded network regions with locally ordered, tetrahedrally coordinated water molecules with almost linear hydrogen bonds and these cooperative order-disorder fluctuations of the random network control the orientational fluctuations of the molecules in supercooled water under low hydrostatic pressure. It is the formation and decay of these ordered, low density regions in the random network of water which leads with decreasing temperature to the rapid increase of the correlation times τ_θ. Application of pressure leads to a distortion of the random hydrogen-bonded network and the liquid is forced to adopt in the time average more compact arrangements with smaller hydrogen-bond angles and with mutual interpenetration of subsections of the random network resulting in an increase of the average number of nearest neighbour molecules. The formation of locally ordered regions in the random network is therefore strongly reduced by hydrostatic pressure. As the topology of the network changes to more compact arrangements with bent hydrogen-bonds, the cooperative order-disorder fluctuations become suppressed by the collective configurational fluctuations dominating the dynamic behaviour of normal viscous liquids. The pressure dependence of the correlation times τ_θ should be enhanced at lower temperatures since in this region the ordered arrays should be more perfectly developed and of a larger size than at higher temperatures so that the "structure breaking" influence of high hydrostatic pressure must become more pronounced. Recently Geiger et al. [36] showed in a molecular dynamics calculation that water at temperatures below room temperature is well above its bond percolation threshold. Liquid water can thus be regarded as a random hydrogen-bonded network which is continuously breaking and reforming under the influence of the thermal motion of the water molecules. Very recently Stanley [37, 38] proposed a correlated site percolation model for the description of supercooled liquid water. In the framework of this model several predictions can be made that can be tested against the results given here:

a) The rotational correlation time τ_θ increases rapidly at the approach of T_H. This agrees with the observed temperature dependence of τ_θ.

b) τ_θ should be longer in D_2O than in H_2O.
The measured isotope effect verifies this prediction.

c) Hydrostatic pressure lowers the correlation times.
This behaviour has been found at temperatures $T \leq 300$ K and pressures $p \leq 200$ MPa and it could be shown that the pressure dependence of τ_θ is stronger in heavy water than in light water.

d) T_s is higher in D_2O than in H_2O.
The T_s-values obtained from Eq. (3) show this isotope effect (see Fig. 7).

e) T_s decreases with increasing pressure much stronger than the melting pressure curve.
This is in agreement with the pressure dependence of T_s obtained (see Fig. 7).

f) The pressure dependence of T_s parallels the pressure dependence of T_H.
Up to $p \simeq 150$ MPa this prediction is in agreement with our results. They indicate however that it may not be the case above $p \simeq 200-250$ MPa (see Fig. 7).

The Stanley model of supercooled liquid water thus accounts qualitatively for most of the experimental findings reported in this paper.

Concluding Remarks

Angell et al. [1] determined a variety of thermodynamic properties of supercooled water and could show that water in its supercooled state has very unusual static properties. The T_1-studies presented here and in two previous reports [3, 4] do reveal that supercooled water also possesses a very anomalous dynamic behaviour. As has been shown by Angell and coworkers, the static response functions seem to be controlled by a thermodynamic singularity at a temperature T_s which lies only a few degrees below the homogeneous nucleation temperature T_H and which, as the T_1-studies showed, is also of relevance for the dynamic behaviour of the molecules in supercooled water at lower pressures. The large density-, energy- and entropy fluctuations corresponding to these static response functions led Speedy and Angell [18] to the suggestion that the anomalies may be due to cooperative order-disorder fluctuations in the random hydrogen-bonded network. The identification of the characteristic frequencies τ_s^{-1} with the hydrogen-bond bending motions which can develop only in the open hydrogen-bonded network with linear hydrogen bonds supports this explanation. Furthermore the measurement of the spin-lattice relaxation times T_1 in $H_2{}^{17}O$ and $D_2{}^{17}O$ revealed a remarkable isotope effect. The correlation times τ_θ of the orientational fluctuations are longer in D_2O than in H_2O. The fact that T_s is higher in D_2O than in H_2O explains the isotope effect observed in the correlation times at low pressures, i.e. at the same reduced temperature ε light and heavy water do show identical dynamic behaviour (see Fig. 8).

With increasing pressure the anomalies vanish and at pressures above $p \simeq 200-250$ MPa liquid water behaves like a normal viscous liquid. The same appears to be true for the static response functions mentioned above which at pressures $p \geq 200$ MPa resemble those of normal polyalcohols [31]. The temperature dependence of the orientational correlation times could be described best in this pressure region by the VTF-equation which includes as a characteristic temperature the ideal glass transition temperature T_0. Increasing pressure lowers T_s very rapidly and it is to be expected that T_s will fall below T_0 at pressure around $200-250$ MPa. This implies, that in supercooled liquid water the cooperative order-disorder fluctuations, characterized by the Speedy-Angell-equation [2] become suppressed in this pressure range and are replaced by the collective configurational fluctuations described by the VTF-equation [3].

The expert technical assistance by Mr. R. Knott and Mr. S. Heyn made this study feasible, their contribution is gratefully acknowledged.

The work presented here was supported by the Deutsche Forschungsgemeinschaft and the Fonds der Chemischen Industrie.

References

[1] C. A. Angell, in: Water – A Comprehensive Treatise, Vol. 7, ed. by F. Franks, Plenum Press, New York 1981, in press.
[2] D. H. Rasmussen and A. P. McKenzie, in: Water Structure and the Water Polymer Interface, ed. by H. H. Jellinek, Plenum Press, New York 1972.
[3] E. Lang and H.-D. Lüdemann, J. Chem. Phys. *67*, 718 (1977).
[4] E. Lang and H.-D. Lüdemann, Ber. Bunsenges. Phys. Chem. *84*, 462 (1980).
[5] G. Völkel, E. Lang, and H.-D. Lüdemann, Ber. Bunsenges. Phys. Chem. *83*, 722 (1979).
[6] U. Gaarz and H.-D. Lüdemann, Ber. Bunsenges. Phys. Chem. *80*, 607 (1976).
[7] A. Abragam, The Principles of Nuclear Magnetism, Oxford University Press, London 1961.
[8] H. W. Spiess, in: NMR Basic Principles and Progress, Vol. 15, ed. by P. Diehl, E. Fluck, and R. Kosfeld, Springer-Verlag, Berlin 1978.
[9] J. A. Glasel, Proc. Natl. Acad. Sci. *58*, 27 (1967).
[10] B. B. Garrett, A. B. Denison, and S. W. Rabideau, J. Phys. Chem. *71*, 2606 (1967).
[11] J. C. Hindman, A. J. Zielen, A. Svirmickas, and M. Wood, J. Chem. Phys. *54*, 621 (1971).
[12] J. C. Hindman, A. Svirmickas, and M. Wood, J. Phys. Chem. *74*, 1266 (1970).
[13] J. C. Hindman, J. Chem. Phys. *60*, 4488 (1974).
[14] T. DeFries and J. Jonas, J. Chem. Phys. *66*, 5393 (1977).
[15] Y. Lee and J. Jonas, J. Chem. Phys. *57*, 4233 (1972).
[16] E. Lang, Dissertation, Universität Regensburg 1980.
[17] W. T. Huntress, Jr., in: Advances in Magnetic Resonance, Vol. 4, ed. by J. S. Waugh, Academic Press, New York 1970.
[18] R. J. Speedy and C. A. Angell, J. Chem. Phys. *65*, 851 (1976).
[19] H. Vogel, Phys. Z. *22*, 645 (1921).
[20] G. Tammann and W. Hesse, Z. Anorg. Chem. *156*, 245 (1926).
[21] G. S. Fulcher, J. Am. Ceram. Soc. *77*, 3701 (1925).
[22] G. Harrison, The Dynamic Properties of Supercooled Liquids, Academic Press, London 1976.
[23] C. A. Angell, J. Chem. Educ. *47*, 583 (1970).
[24] J. Wong and C. A. Angell, Glass-Structure by Spectroscopy, Marcel Dekker Inc., New York 1976.
[25] M. H. Cohen and D. Turnbull, J. Chem. Phys. *31*, 1164 (1959).
[26] M. H. Cohen and G. S. Grest, Phys. Rev. B *20*, 1077 (1979).
[27] G. Adam and J. H. Gibbs, J. Chem. Phys. *43*, 139 (1965).
[28] C. A. Angell and E. J. Sare, J. Chem. Phys. *52*, 1058 (1970).
[29] H. Kanno and C. A. Angell, J. Phys. Chem. *81*, 2639 (1977).
[30] M. Sugisaki, H. Suga, and B. Seki, Bull. Chem. Soc. Jpn. *41*, 2591 (1968).
[31] H. Kanno and C. A. Angell, J. Chem. Phys. *73*, 1940 (1980).
[32] H. Kanno, J. Shirotani, and S. Minomura, Bull. Chem. Soc. Jpn. *53*, 2079 (1980).
[33] G. E. Walrafen, in: Water – A Comprehensive Treative, Vol. 1, ed. by F. Franks, Plenum Press, New York 1972.
[34] A. Korosi and B. M. Fabuss, Anal. Chem. *40*, 157 (1968).
[35] M. A. Anasimov, A. V. Voronel, N. S. Zangol'nikova, and G. J. Ovodov, JETP Lett. *15*, 317 (1972).
[36] A. Geiger, F. H. Stillinger, and A. Rahman, J. Chem. Phys. *70*, 4185 (1979).
[37] H. E. Stanley, J. Phys. *A 12*, 329 (1979).
[38] H. E. Stanley and J. Teixeira, J. Chem. Phys. *73*, 3404 (1980).
[39] P. Thaddeus, L. C. Krisher, and T. H. N. Loubser, J. Chem. Phys. *40*, 257 (1964).

[40] J. Verhoeven, A. Dymanus, and H. Bluyssen, J. Chem. Phys. *50*, 3330 (1969).
[41] D. T. Edmonds and A. Zussman, Phys. Lett. *41A*, 167 (1972).
[42] O. Lumpkin and W. T. Dixon, Chem. Phys. Lett. *62*, 139 (1979).
[43] D. T. Edmonds and A. L. Mackay, J. Magn. Reson. *20*, 515 (1975).
[44] P. Waldstein, S. Rabideau, and J. A. Jackson, J. Chem. Phys. *41*, 3407 (1964).
[45] H. W. Spiess, B. B. Garrett, R. K. Sheline, and S W. Rabideau, J. Chem. Phys. *51*, 1201 (1969).
[46] H. Kanno and C. A. Angell, J. Chem. Phys. *70*, 4008 (1979).
[47] M. Oguni and C. A. Angell, J. Chem. Phys. *73*, 948 (1980).
[48] J. Jonas, T. DeFries, and D. J. Wilbur, J. Chem Phys. *65*, 582 (1976).

(Eingegangen am 26. Februar 1981, E 4873
endgültige Fassung am 18. März 1981)

Laser-Blitzlichtphotolytische Untersuchungen zur Druckabhängigkeit der Reaktion $ClO + NO_2 + N_2 \rightarrow ClONO_2 + N_2$

W. Dasch, K.-H. Sternberg und R. N. Schindler

Institut für Physikalische Chemie, Universität Kiel, Olshausenstraße 40 – 60, D-2300 Kiel 1

Freie Radikale / Gase / Photochemie / Reaktionskinetik

The kinetics of the reaction $ClO + NO_2 + N_2 \rightarrow ClONO_2 + N_2$ was investigated at room temperature in the pressure range $28 < p < 824$ mbar by ClO-absorption measurements. As source for ClO radicals Cl_2O was used. The reaction was initiated using monochromatic light pulses from a KrF*-excimer laser at $\lambda = 248.5$ nm. A Xe-high pressure lamp and a pulsed Mg-hollow cathode lamp respectively were used as analytic light sources. The atomic emission of the hollow cathode source at $\lambda = 285.2$ nm coincides with the 8. vibrational state of the ClO absorption. The results are discussed and compared with data obtained in other experimental studies as well as in model calculations.

I. Einleitung

Nach bisherigen Modellberechnungen führen Chloratome, die zu einem wesentlichen Anteil aus der Photolyse der Freone stammen, in der Stratosphäre zur katalytischen Zersetzung von Ozon. Bildung von Chlornitrat, $ClONO_2$, in der Atmosphäre könnte den Ozonabbau verlangsamen, da in diesem Produkt ein Teil des aktiven Kettenträgers Chlor gebunden ist [1]. Zur Berücksichtigung dieser Schutzfunktion durch $ClONO_2$-Bildung in Modellrechnungen sind kinetische Informationen zur Bildung und zur Zersetzung von Chlornitrat unter atmosphärischen Bedingungen von Bedeutung.

Der vorliegende Bericht über Untersuchungen zur Druckabhängigkeit der $ClONO_2$-Bildungsgeschwindigkeit basiert auf einer blitzspektroskopischen Studie unter Verwendung eines KrF*-Excimeren-Lasers. Als ClO-Radikalquelle wurde Dichlormonoxid Cl_2O eingesetzt. Der Druck des chemisch inerten dritten Stoßpartners Stickstoff wurde im Bereich 26 – 822 mbar variiert. Wegen des kleinen Absorptionskoeffizienten von NO_2 für das Photolysenlicht kann sichergestellt werden, daß >99% der absorbierten Strahlung zur Zersetzung des Dichlormonoxids dient.

Die durch Photodissoziation von Cl_2O ausgelösten Reaktionsschritte führen zur Chlornitratbildung nach dem folgenden Reaktionsschema (1) – (3).

$$Cl_2O + h\nu(\lambda = 248.5\,\text{nm}) \rightarrow Cl + ClO \quad (1)$$

$$Cl + Cl_2O \rightarrow Cl_2 + ClO \quad (2)$$

$$ClO + NO_2 + N_2 \rightarrow ClO \cdot NO_2 + N_2\,. \quad (3)$$

Aussagen zur Geschwindigkeit der Chlornitratbildung (3) werden aus der Abnahme von [ClO] als Funktion von $[NO_2]$ und $[N_2]$ erhalten.

Die bisherigen Kenntnisse zur Geschwindigkeit der Chlornitratbildung stammen im wesentlichen aus 3 Gruppen von sehr unterschiedlichen Experimenten: Zur ersten Gruppe gehören 3 unabhängige Untersuchungen, die in Strömungssystemen im Niederdruckbereich bis 8 mbar N_2 durchgeführt wurden. Zahniser et al. [2] verfolgten die Reaktion (3) durch indirekte Messungen der ClO-Konzentration. Bei Zugabe von NO wurde ClO quantitativ in Cl-Atome umgewandelt, die durch Resonanzfluoreszenz bei 134,7 nm nachgewiesen wurden. Leu et al. [3] sowie Birks et al. [4] benutzten Massenspektrometer in ihren Anordnungen zur Messung von ClO-Konzentrationen. Alle drei Untersuchungen blieben auf den Niederdruckbereich beschränkt.

Die zweite Gruppe von Experimenten umfaßt IR-spektroskopische Untersuchungen zur thermischen Zersetzung von Chlornitrat [5] bzw. zum thermisch induzierten Austausch zwischen $ClONO_2$ und $^{15}NO_2$ [6] im Druckbereich bis 460 bzw. 160 mbar N_2. Die hier erhaltenen kinetischen Daten erlaubten die Berechnung von k_3 mit Hilfe der Gleichgewichtskonstanten für das Gleichgewicht

$$ClONO_2 \rightleftharpoons ClO + NO_2 \quad (4)$$

sowie des Arrheniusparameters.

Zur dritten Gruppe von Experimenten gehört eine kinetische Untersuchung zur Druck- und Temperaturabhängigkeit von Reaktion (3) mit Hilfe der modulierten Photolyse von Cl_2/Cl_2O-Gemischen [7] und die vorliegende blitzphotolytische Untersuchung. In beiden Experimenten wird die Reaktion (3) durch optische Messungen am intermediären ClO verfolgt. Der Druckbereich bis >800 mbar wird überstrichen.

Während in allen Experimenten der Gruppen 1 und 3 das Verschwinden der Radikale ClO messend verfolgt wurde, wobei